

**RECENT DEVELOPMENTS IN METAL BASED PHOTOCATALYSTS – A REVIEW****V. Nithya, A. Loganathan, P. Mahalingam and P. Sivakumar\****Department of Chemistry, Arignar Anna Government Arts College, Namakkal – 637 002, (Tamilnadu) India**\*Corresponding author: shivagobi@gmail.com***ABSTRACT**

The problem of fresh water scarcity is growing all around the world due to the over utilization and pollution. Discharge of pollutants especially dye bearing wastewater drastically affects the life of flora and fauna. Finding a suitable technology for the treatment of wastewater is highly warranted in the present context. Photocatalytic degradation using metal and metal oxide composite has lot of advantages like negligible by-products, simple to operate and economically very cheap. This manuscript reviews the potential photocatalytic applications of Ti, V, Mn, Co, Cu, Zn, Ga, Zr, Pd, Sn and inner transition metal doped catalysts.

**Keywords:** Photocatalysis, Band gap, Dyes, Semiconductor, Doping

**1. INTRODUCTION**

Environmental problems especially the pollution of water by various organic and metallic ion has a great impact on the sustenance of life on the earth. Especially in India various dyes bearing waste water is drained into rivers without satisfactory treatment. This causes serious environmental problems such as increase of toxicity chemical oxygen demand (COD), biochemical oxygen demand (BOD), bad smell and color to the aquatic environment. The problem of contaminated water can be effectively solved by photocatalytic process through removal of impurities. Photocatalysis play important role in maintaining the environment quality by the way of pollution abatement. Heterogeneous photocatalysis is a widely accepted technique of choice for removal of wide variety of complex organic contaminants with lesser by products.

The photocatalysis is the addition of light to semiconductor oxide/sulphide that results in electron moving from the valence band to conduction band. The electron hole pairs formed will react with oxygen and water molecules to create superoxide anions and hydroxide radical. The superoxide anions and hydroxide radicals increases the reducing and oxidizing abilities which can be used for the treatment of wide variety of industrial effluents. Semiconductor photocatalysts are widely used for complete mineralization of organic pollutants into less harmful byproduct such as H<sub>2</sub>O, CO<sub>2</sub>, and mineral acids. Several types of promising photocatalysts such as titanium dioxide, zinc oxide, iron(III) oxide, zirconia, vanadium(V) oxide, niobium

pentoxide and tungsten trioxide etc have been actively applied in environmental waste management system.

TiO<sub>2</sub> and ZnO have been widely applied as photocatalyst due to their high activity, non toxicity, chemical stability, lower costs, optical and electrical properties and environment friendly characteristics. The catalyst reduced to the nanoscale can demonstrate different properties compared to properties at macroscale size, facilitating unique applications in photocatalyst degradation of organic waste. Nano photocatalysts have been intensively examined because of their increased surface area which sturdily influences their physiochemical properties.

Doped and composite nanostructure metal oxides have been considered as an interesting material and have shown excellent properties in photocatalysis. Doping of nanomaterials modifies their features and characteristics. Nano composites generally increase numerous properties of metal oxide to fulfill the growing demand for various applications. Doping and nano composition improve the surface area and reduce the size of the metal oxide nano structure. Doping of nano material also tunes the band gap energy and enhances the conductivity, electrical, mechanical, barrier, sensing and solar photocatalytic properties.

Efficiency of the prepared photocatalyst for the degradation of organic effluent is greatly influenced by various parameters, starting from synthesis of nanocatalyst up to the operating conditions of effluent degradation. The good photocatalytic activity of these metal oxides was used for hydrogen production through water splitting / decomposition of water pollutants. One

more advantage of photocatalysis over other existing technology is that there is no requirement of secondary disposal.

This review analyses the various preparation methods and photocatalytic applications of metal oxides/composite metal oxides photocatalysts such as titanium dioxide, vanadium, manganese, cobalt, copper, zinc, gallium, zirconium, palladium, and other lanthanum transition metal based photocatalysts.

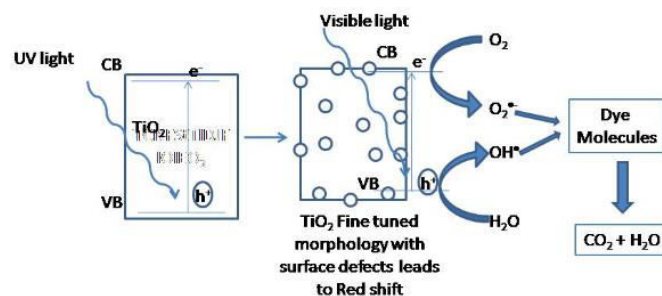
## 2. TiO<sub>2</sub>PHOTOCATALYSIS

TiO<sub>2</sub> is a well-known semiconductor material for the effective photocatalysis. There are thousands of papers being published every year based on TiO<sub>2</sub>. The only problem associated with TiO<sub>2</sub> is its poor activity under visible light as well as frequent electron hole recombination. To overcome these limitations, there are many researches being carried out to fine tune the band gap. The subsequent paragraphs will review latest developments in TiO<sub>2</sub> based photocatalysts.

Watson et al (2004) studied the preparation of nanosized crystalline TiO<sub>2</sub> particles at low temperature for photocatalysis [1]. They prepared nanocrystalline titania particles using titanium isopropoxide as the precursor in an acidic medium by a modified alkoxide process. They observed that at lower reaction temperature, rutile was favored whilst at a higher reaction temperature anatase and brookite were formed. Moreover anatase and rutile particles were prepared by the conventional alkoxide method at high calcinations temperature of 450 and 900°C respectively. The photocatalytic activity of the prepared particles was tested for the degradation of sucrose. The photocatalytic activities of the prepared nanosized TiO<sub>2</sub> were compared to Degussa P-25. At low organic concentrations, Degussa P-25 exhibited higher photocatalytic behavior than all the prepared particles while, at high organic concentrations, the nanosized TiO<sub>2</sub> particles displayed an activity comparable to Degussa P-25. The high photoactivity of the particles prepared by the modified alkoxide method was explained in terms of the availability of active sites which may be favourable for reduction of organics. They also observed the photocatalytic mineralization rate of sucrose by Degussa P-25 was suspected to be strongly influenced by the intermediates at high organic concentration while the prepared particles were not.

Liao and Liao (2007) studied the shape, size and photocatalytic activity control of TiO<sub>2</sub> nanoparticles with surfactants [2]. They synthesized the shape, size and photocatalytic activity controlled TiO<sub>2</sub> nanoparticles

from Ti(OBu)<sub>4</sub> and TiCl<sub>3</sub> through the sol-gel method. The photocatalytic activity of prepared TiO<sub>2</sub> nanoparticles was evaluated in fixed film batch reactors using methyl orange as a model compound. They suggested the different morphologies of TiO<sub>2</sub> nanoparticles with the use of different surfactants and titanium precursors and all the nanoparticles were calcined at 500°C. Uniform spherical and cubic TiO<sub>2</sub> nanoparticles were obtained when DBS and SDS or cellulose was used respectively and also short TiO<sub>2</sub> nanorods were observed when cellulose was used. They observed the shape controlled TiO<sub>2</sub> nanoparticles have a lower band gap than the neat anatase TiO<sub>2</sub> nanoparticles and P-25. The red shift of light reflectance of shape-controlled nanoparticles could be due to a large amount of surface defects on particle surfaces which make the shape-controlled nanoparticles have a higher ability to capture electron-hole pairs. Moreover number of active sites, surface defects and adsorption properties of shape and size controlled TiO<sub>2</sub> nanoparticles, might also be responsible for the higher photocatalytic activity. They also referred TiO<sub>2</sub> nanoparticles with different shapes and sizes showed different photocatalytic activities and cubic nanoparticles prepared with the use of SDS had a higher photocatalytic activity than other TiO<sub>2</sub> nanoparticles.



The photocatalytic activity of TiO<sub>2</sub>:AlPO<sub>4</sub>-5 zeolite for the degradation of indigo carmine dye was studied by Suresh Kumar et al (2010) [3]. They prepared aluminophosphate zeolite coated/impregnated by clusters of TiO<sub>2</sub> under hydrothermal conditions. They clearly proved the TiO<sub>2</sub> particles are coated and impregnated in the cages of AlPO<sub>4</sub>-5 zeolites. They also studied the average specific surface area of the AlPO<sub>4</sub>-5 zeolites (54.05 m<sup>2</sup>g<sup>-1</sup>) is strongly dependent on the percentage weight of TiO<sub>2</sub> and decrease in the surface area of TiO<sub>2</sub>:AlPO<sub>4</sub>-5 (9.12 m<sup>2</sup>g<sup>-1</sup>) is because of the entry of TiO<sub>2</sub> particles into the pores and channels and blocking the same. They also studied the TiO<sub>2</sub>:AlPO<sub>4</sub>-5 shows high photocatalytic efficiency when compared to TiO<sub>2</sub> alone with dye concentration was maintained constant. The amount of the catalyst was varied between 10 and 30

mg in 50 mL of the aqueous dye solution and the degree of decolourisation and decomposition of the dye solution increases with an increase in the amount of catalyst, and the highest efficiency was attained at 29 mg / 50 mL. An increase in the decomposition efficiency is due to the increase in the number of active sites in  $\text{TiO}_2:\text{AlPO}_4\text{-5}$  composites available for the reaction, which in turn increases the rate of radical formation. They explained  $\text{TiO}_2$  present in the composite completely mineralized the organics trapped by the  $\text{AlPO}_4\text{-5}$  and the organics present in the dye solution there by making the  $\text{TiO}_2:\text{AlPO}_4\text{-5}$  composite as an efficient photocatalyst.

$\text{TiO}_2$  nanoparticles loaded on graphene/carbon composite nanofibers by electrospinning for increased photocatalysis was studied by Chang Hyo Kim et al (2012) [4]. The authors have deposited small  $\text{TiO}_2$  nanoparticles on electrospun CCNFs by the sol-gel method and these composites were very active photocatalysts in the photodegradation of methylene blue under visible light irradiation. The high migration efficiency of photo induced electrons and the inhibition of charge-carrier recombination due to the electronic interaction between  $\text{TiO}_2$  and graphene. They suggested that the graphene acts as an electron acceptor and a photosensitizer, which causes an increase in the photodegradation rate and reduces electron-hole pair recombination. They also reported that  $\text{TiO}_2\text{-CCNF}$  has a higher efficiency for the decomposition of MB than the  $\text{TiO}_2\text{-CNF}$ , CCNF and CNFs and the introduction of graphene and CNFs to the  $\text{TiO}_2$  photocatalyst could increase the decomposition rate of some organic compounds using a photocatalytic process. The  $\text{TiO}_2\text{-CCNF}$  materials could be used for multiple degradation cycles without a decrease in photocatalytic activity.

Though  $\text{TiO}_2$  has plenty of scope to be used as photocatalyst, still a long way to go for effective implementation of  $\text{TiO}_2$  in large scale industrial operation.

### 3. VANADIUM BASED PHOTOCATALYSIS

The limitations of  $\text{TiO}_2$  application tempts the researchers to go for an alternate photocatalyst. The vanadium oxide and its composites also have a promising future if it is properly fabricated. The subsequent paragraphs review the various preparative methods of vanadium oxides and their applications.

Benxia Li et al (2006) studied the vanadium pentoxide nanobelts and nanorolls; from controllable synthesis for the investigation of their electrochemical properties and photocatalytic activities [5]. They synthesized uniform

$\text{V}_2\text{O}_5 \cdot x\text{H}_2\text{O}$  nanobelts and nanorolls with very high aspect ratios on a large scale through a facile hydrothermal route in the presence of sulfuric acid or acetic acid. They observed the nanobelts are tens of micrometres long, 100-150nm wide and 20-30nm thick. They proposed the nanobelts and nanorolls were layered structure of vanadium pentoxide. They prepared hydrous and anhydrous  $\text{V}_2\text{O}_5$  nanostructure, which exhibit good photocatalytic degradation abilities on Rhodamine-B. They reported  $\text{V}_2\text{O}_5 \cdot 0.6\text{H}_2\text{O}$  nanorolls exhibit better electrochemical capacitance and photocatalytic activity, larger surface area and lower water content than the former. They also investigated the electrochemical intercalation properties with  $\text{Li}^+$ .

The nanostructured  $\text{VO}_2$  photocatalysts for hydrogen production was studied by Yuquan Wang et al (2008) [6]. They evaluated the photocatalytic property of the vanadium oxide nano structures by measuring the hydrogen evolution from a mixture of water and ethanol under UV light at room temperature. They reported a new crystal structure for nanostructured  $\text{VO}_2$ , with bodycenterd-cubic structure with a lattice constant of  $\sim 0.94$  nm and the optical band gap of the bcc  $\text{VO}_2$  is 2.7 eV which is much larger than the value of 0.7 eV for monoclinic  $\text{VO}_2$ . They observed bcc  $\text{VO}_2$  exhibit excellent photocatalytic activity with a quantum efficiency of 38.7% in hydrogen generation by photo assisted water splitting. They also achieved hydrogen production rate of  $\sim 800$  mmol/m<sup>2</sup>/h under 500W mercury light.

Yim-Leng Chan et al (2014) studied the synthesis of  $\text{V}_2\text{O}_5$  nanoflakes on PET fiber as visible-light driven photocatalysts for degradation of RhB dye [7]. They successfully synthesized  $\text{V}_2\text{O}_5$  nanoparticles and  $\text{V}_2\text{O}_5$  nanoflakes by sol-gel method. They suggested  $\text{V}_2\text{O}_5$  nanoparticles are visible light driven semiconductor photocatalysts. The  $\text{V}_2\text{O}_5$  nanoparticles were rod-like with average length of  $231.9 \pm 14.9$  nm and thickness of the nanoflakes in the range of 5-20 nm. The photocatalytic activities for both  $\text{V}_2\text{O}_5$  nano particles and  $\text{V}_2\text{O}_5$  nanoflakes grown on fiber were  $0.0149 \text{ min}^{-1}$  and  $0.0065 \text{ min}^{-1}$  respectively under visible light irradiation. They indicated both  $\text{V}_2\text{O}_5$  nanostructures used as visible-light driven photocatalysts to remove organic pollutants. They proposed photodegradation of  $\text{V}_2\text{O}_5$  nanostructures to degrade RhB dye under visible light irradiation. They reported the bond edge of valence band (2.81eV), which is more positive than the oxidation potential of  $\text{H}_2\text{O}$  (1.99eV) this is able to produce OH free radicals. These

free radicals responsible for the degradation of RhB dye into less harmful by product.

The silver vanadium oxide nanomaterial through controlled synthesis by hydrothermal method and efficient photocatalytic degradation of atrazine and CV dye was reported by Chiing-Chang C et al (2017) [8]. They observed the band gap values for all silver vanadate samples in the range of 1.85-2.25 eV. They reported silver vanadate catalyst have high photocatalytic activity, which degraded nearly 100% of CV from the solution after 24h under visible light irradiation and 97% of Atrazine was degraded after 72 h. They evaluated the potential degradation pathways exhibits two different degradation pathways including dechlorination-hydroxylation, alkylic-oxidation de-alkylation. They observed the N-de-methylation of the CV dye takes place in a stepwise manner with the various N-de-methylated intermediate CV species. They also observed the excellent activity and photostability reveal that silver vanadate is a promising visible light responsive photocatalyst for water and waste water treatment.

The photocatalytic studies of vanadium based catalysts have reported effective important in the band gap. The applicability these catalyst and its composites are still to be studied.

#### 4. MANGANESE BASED PHOTOCATALYSTS

Nano structure metal oxide semiconductors have attracted great attention in recent years due to their exceptional electronic, optical, electrochemical and sensing properties.  $\text{MnO}_2$  has attracted intensive interest because of its low cost, environmental compatibility and abundant availability.  $\text{MnO}_2$  can offer opportunities for many applications related to Li-ion batteries, super capacitors, gas sensors and catalysts. The subsequent paragraphs review the latest developments in manganese based photocatalysts.

Bosi Yin et al (2014) studied the facile synthesis of ultralong  $\text{MnO}_2$  nanowires as high performance supercapacitor electrodes and photocatalysts with enhanced photocatalytic activities [9]. They synthesized ultralong  $\text{MnO}_2$  nanowires by a simple one-step solution system. They suggested ultralong  $\text{MnO}_2$  nanowires with a large BET surface area and narrow size distribution which exhibits ideal capacitor behavior and complete degradation of organic dye molecules. They reported that the electrochemical measurements of nanowires offer many advantages in performance such as high specific capacitance, good charge-discharge stability, long-term cycling life, and low leakage current. They determined

the ultralong  $\text{MnO}_2$  nanowire architecture provides a shortened diffusion path for electrons and ions. They also suggested the synthesized  $\text{MnO}_2$  nanowires exhibit excellent photocatalytic toward MO, Eosin red and CR. They reported two ways to enhance the photocatalytic efficiency of  $\text{MnO}_2$  nanowires. First one is decrease in the recombination of the photogenerated electrons and holes allow them to take part in the photocatalytic reaction. Second one is optimizing the morphology and structure of the products, which can lead to more reactive species, thus the photocatalytic efficiency can be enhanced. They also reported  $\text{MnO}_2$  nanowire formation may be attributed to the ultralong and mesoporous structure. This structure can provide more active sites to adsorb reactive species and  $\text{O}_2$  and allow more effective transport for the reactant molecules to get to the active sites.

Safi Asim Bin Asif et al (2015) studied the visible light active photocatalyst based on  $\text{Al}_2\text{O}_3$  doped  $\text{Mn}_3\text{O}_4$  nanomaterial for the degradation of organic toxin [10]. They synthesized  $\text{Al}_2\text{O}_3$  doped  $\text{Mn}_3\text{O}_4$  nanomaterial by low-temperature stirring method. They evaluated photocatalytic activity of  $\text{Al}_2\text{O}_3$  doped  $\text{Mn}_3\text{O}_4$  multi-metal oxide nanoparticles through degradation of BCB under visible light irradiation. They observed the band gap energy of  $\text{Al}_2\text{O}_3$  doped  $\text{Mn}_3\text{O}_4$  materials is around 1.82 eV and pure  $\text{Mn}_3\text{O}_4$  band gap energy is found to be 5.30 eV. They also observed that the metal oxide shows efficient activity for degradation of BCB dye at different pH under solar light irradiation. They showed singlet oxygen and hydroxyl radicals generated by oxidation and reduction reaction of  $\text{O}_2$  and  $\text{H}_2\text{O}$  respectively and continued attacks of  $\text{O}_2^{\cdot-}$  and  $\cdot\text{OH}$  radicals on pollutant species lead to the degradation of the dye molecule. They also reported the decay of BCB follows the pseudo first order kinetics which satisfied the Langmuir – Hinshelwood (L-H) kinetic method.

The synthesis, characterization and photocatalytic activity of  $\text{MnO}_2/\text{Al}_2\text{O}_3/\text{Fe}_2\text{O}_3$  nanocomposite for degradation of malachite green was studied by Haile Hasana Logita (2015) [11]. They synthesized nanocomposite  $\text{MnO}_2/\text{Al}_2\text{O}_3/\text{Fe}_2\text{O}_3$  photocatalyst by sol-gel method using metal salts as precursors in the presence of acid catalyst. They suggested that the synthesized nanopowders have a crystal structure with a size range of 20 to 26 nm. They evaluated photocatalytic activity of  $\text{MnO}_2/\text{Al}_2\text{O}_3/\text{Fe}_2\text{O}_3$  through degradation of MG dye. The reported band gap energy was about 1.97 eV which is an important band gap for improving photocatalytic

degradation of organic dyes in the visible region. They also reported the higher decolourization efficiency was obtained under visible light irradiation in the presence of the catalyst.

Manoj Pudukudy and Zahira Yaakob (2016) studied the synthesis, characterization and photocatalytic performance of mesoporous  $\alpha$ - $\text{Mn}_2\text{O}_3$  microsphere prepared via a precipitation route [12]. They prepared  $\alpha$ - $\text{Mn}_2\text{O}_3$  microspheres with high phase purity, crystallinity and surface area by the thermal decomposition of precipitated  $\text{MnCO}_3$  microspheres without the use of any structure directing agents and tedious reaction conditions. They investigated the photocatalytic activity of  $\text{Mn}_2\text{O}_3$  microsphere by MB under UV light irradiation. They reported porous semi conductors with high surface area have a great role in photocatalysis and applicability for the wastewater treatment. They confirmed the formation of bcc phase crystalline structure of  $\text{Mn}_2\text{O}_3$  without any other impure phase by the powder XRD analysis. The measured specific surface area is found to be  $32 \text{ m}^2/\text{g}$  with mono modal mesoporous texture. They reported  $\text{Mn}_2\text{O}_3$  microspheres shows a moderate photocatalytic activity of 38% for the degradation of MB dye over a low catalyst dose of 0.05g using air as the oxidizing agent. Manganese in its highest oxidation state is well known for its oxidation capacity. But these studies indicated that at lower oxidation state and codoping with other entities makes manganese oxide are efficient photocatalyst for the solar energy harvesting purposes.

## 5. COBALT BASED PHOTOCATALYSIS

Cobalt oxide nano materials have shown much application in different sectors. They have been used in Li-ion battery, catalysis and sensing applications. All these properties depend on the particle size of cobalt. The following paragraphs review the various preparative methods of cobalt based catalysis and their applications.

Christoffer Johans et al (2008) studied the control of particle size by pressure adjustment in cobalt nanoparticle synthesis [13]. They synthesized cobalt nanoparticles by a novel pressure drop-induced decomposition method. The supersaturation during the thermal decomposition of  $\text{Co}_2(\text{CO})_8$  is directly controlled via the CO pressure and the supersaturation affects the nucleation rate and particle size. They observed at a decomposition pressure of 3.2 bar and the synthesis produced even bigger particles, with a diameter of approximately 31 nm, which cluster readily on the grid. Particles of 81 and 139 nm were obtained at

decomposition pressures of 4.5 and 5.5 bar respectively and also cobalt nanoparticle indicated the multicrystalline nature of the particle. They also analyzed the growth rates of the particles by correlating the CO released in the synthesis to a model based on kinetically controlled growth following instantaneous nucleation.

The efficient solar photocatalyst based on cobalt oxide / iron oxide composite nanofibers for the detoxification of organic pollutants was studied by Safi Asim Bin Asif et al (2014) [14]. They prepared well crystalline  $\text{Co}_3\text{O}_4/\text{Fe}_2\text{O}_3$  composite nanofibers by a low-temperature process. They evaluated the photocatalytic property of the composite nanofibers by using toxic dyes AO and BCB under solar light. They suggested the composite nanofibers are metal oxide-based nanostructures. The band gap energy of the composite nanofibers is found to be 2.12 eV. They investigated the photocatalytic degradation of dye by pH in the range of 7 to 10 and 0.1 g composite nanofiber under solar light irradiation. Photocatalytic degradation of acridine orange dye increased with increasing the pH 7.0 to 10.0 in visible light. They observed visible light enhances the charge transformation on the surface of the composite nanofibers and results in hydroxyl radical formation which facilitates the degradation. They reported that the nanofibers are active photocatalyst for achieving capable photocatalysts in favour of water resources and health observation.

David Greene et al (2014) studied the synthesis, characterization and photocatalytic studies of cobalt ferrite-silica-titania nanocomposites [15]. They prepared and coated magnetic cobalt ferrite nanoparticles by the double  $\text{SiO}_2/\text{TiO}_2$  layer using metallorganic precursors to give new functional "core-shell" nano-structures. They showed a reduction in magnetic moment and the size of the non-magnetic coating has increased due to the presence of non-magnetic  $\text{TiO}_2$  shell, resulting in a lower magnetic moment. The main coating around the core is a  $\text{SiO}_2$  shell of approximately 50 nm thick. Then second  $\text{TiO}_2$  coating lies on top of the silica shell. They demonstrated that the sintering of  $\text{CoFe}_2\text{O}_4@\text{SiO}_2@\text{TiO}_2$  at  $600^\circ\text{C}$  allows them to produce photocatalytically active anatase and rutile forms of  $\text{TiO}_2$ . They tested photocatalytic activity of  $\text{CoFe}_2\text{O}_4@\text{SiO}_2@\text{TiO}_2$  core-shell nanoparticles to the methylene blue solution, the absorbance of the dye reduced much faster as opposed to the control tests. They demonstrated the  $\text{CoFe}_2\text{O}_4@\text{SiO}_2@\text{TiO}_2$  nanoparticles of the catalyst totally recoverable from the

reaction mixture using a simple magnetic separation using a permanent magnet.

The highly efficient and selective photocatalytic CO<sub>2</sub> reduction by iron and cobalt quarter pyridine complexes was studied by Zhenguo Guo et al (2016) [16]. They reported highly efficient and selective photocatalytic reduction of CO<sub>2</sub> by cobalt (II) and iron (II) complexes bearing a quaterpyridine ligand. They investigated the photocatalytic reduction of CO<sub>2</sub> by [Co(qpy)(OH<sub>2</sub>)<sub>2</sub>]<sup>2+</sup> and [Fe(qpy)(OH<sub>2</sub>)<sub>2</sub>]<sup>2+</sup>. They used Ru(bPy)<sub>3</sub><sup>2+</sup> as the photosensitizer and 1,3-dimethyl 1,2-phenyl-2,3-dihydro-1 H-benzo[d] imidazole (BIH) as the sacrificial reductant in CH<sub>3</sub>CN/TEDA solution under visible light excitation. They determined quantum yields for CO production by ferric oxalate actinometry. The quantum yield for the overall photocatalytic reduction of CO<sub>2</sub> and CO is 2.8% and 8.8% after irradiation for 12 h at 458nm.

## 6. COPPER BASED PHOTOCATALYSIS

Several transition metal oxides have been shown to catalyze the water splitting reaction, usually in the presence of a metal or metal oxide co-catalyst and sometimes with sacrificial agents in solution. For solar water splitting, Cu<sub>2</sub>O possesses favorable energy-band positions; the potential of its conduction band is 0.7 V lower than the hydrogen evolution potential and that of its valence band is slightly higher than the oxygen evolution potential. The subsequent paragraphs review the various preparative methods of copper based photocatalysts and applications.

Rashed et al (2012) studied the magnetic and catalytic properties of cubic copper ferrite nanopowder synthesized from secondary resources [17]. They synthesized cubic copper ferrite by hydrothermal method at different temperatures from 100 to 200°C for times from 12 to 36 h with pH values 8-12. They observed the average crystallite size was decrease by increasing the temperature and the average crystallite size of produced copper ferrite powders range from 24.6 nm to 51.5 nm. They also studied photocatalytic activity of cubic copper ferrite by degradation of the methylene blue from aqueous solution. Cubic copper ferrite powders from the industrial waste were used as W/W (waste for treatment of other waste). They reported the catalytic efficiency was 95.9% at hydrothermal temperature 200°C for hydrothermal time 24h at pH 12 with high surface area of 118.4m<sup>2</sup>/g.

The copper (I) oxide nanocrystals – one step synthesis, characterisation, formation mechanism and

photocatalytic properties was studied by Anshu Singhal et al (2013) [18]. They synthesized Cu<sub>2</sub>O nanocrystals under mild conditions by simple one pot synthesis routes with inexpensive starting materials. They suggested two preparation methods a). Thermal decomposition of copper-organic precursors copper (II) acetate or copper (II) acetylacetonate in long chain organic solvents oleyl alcohol and trioctylamine respectively, at 170°C and b). A surfactant-free solvothermal approach involving the reaction of copper (II) acetylacetonate in acetone at 140°C. They observed Cu<sub>2</sub>O-OLOH and Cu<sub>2</sub>O-ST found to be pure cubic phase. The BET surface areas and maximum pore radii values for the different Cu<sub>2</sub>O nanocrystals are 55 m<sup>2</sup>g<sup>-1</sup> and 90-92 Å for Cu<sub>2</sub>O-OLOH, 105 m<sup>2</sup>g<sup>-1</sup> and 40-42 Å for Cu<sub>2</sub>O-TOA and 65 m<sup>2</sup>g<sup>-1</sup> and 100 Å for Cu<sub>2</sub>O-ST respectively. They suggested oleyl alcohol and trioctylamine play dual roles as solvents and mild reductants by reducing Cu (II) to Cu (I) species during the course of thermal decompositions of copper-organic precursors. They evaluated the photocatalytic properties of the Cu<sub>2</sub>O nanocrystals by hydrogen generation from water/methanol (2:1) mixtures under UV/visible irradiation (16% UV + 84% visible). The overall trend of photocatalytic activity is Cu<sub>2</sub>O-OLOH < Cu<sub>2</sub>O-ST = Cu<sub>2</sub>O-TOA.

Shabana Afzal et al (2013) studied the photostable self-cleaning cotton by a copper (II) porphyrin/TiO<sub>2</sub> visible-light photocatalytic system [19]. They prepared thin films of meso-tetra (4- carboxyphenyl) porphyrinato copper (II) (CuTCPP) in conjunction with anatase TiO<sub>2</sub> on cotton fabric. They investigated self-cleaning properties by conducting photocatalytic degradation of methylene blue, coffee and wine stains under visible light irradiation. They observed CuTCPP/TiO<sub>2</sub>-coated cotton fabrics shows superior self-cleaning performance when compared to bare TiO<sub>2</sub>- coated cotton. They also observed CuTCPP/TiO<sub>2</sub> coated fabrics shows significant photostability under visible-light compared to free base TCPP/TiO<sub>2</sub>-coated fabrics. They also reported the enhanced photo stability of CuTCPP shows good potential in view of reproducibility and practical application of self-cleaning textiles.

The green synthesis of colloidal copper oxide nanoparticles using Carica papaya and its application in photocatalytic dye degradation was reported by Renu Sankar et al (2013) [20]. They green synthesized copper oxide nanoparticles by treating 5mM cupric sulphate with carica papaya leaves extract. They investigated photocatalytic activity of green synthesized copper oxide

nanoparticles by coomassie brilliant blue R-250 dye under bright sunlight. They observed the incubation time of nanoparticles was increased, the rates of decolorization of dye also increased. They also observed green synthesized copper oxide nanoparticles are rod in shape and having a mean particle size of 140nm, further negative zeta potential disclose its stability at -28.9 mV. They reported the color dye degradation is mainly accredited to the size, morphology and surface charge property of the green synthesized copper oxide nanoparticles.

The controlled synthesis of  $\text{Cu}_2\text{O}$  nano crystals with uniform morphology has become an important issue. Furthermore  $\text{Cu}_2\text{O}$  is an inexpensive, plentiful, and readily available and has low toxicity and good environmental acceptability, which favors the fundamental and practical research on  $\text{Cu}_2\text{O}$ . Cu catalysis have attractive properties, various methods both physical and chemical have been developed for the synthesis of 0D, 1D and 2D  $\text{Cu}_2\text{O}$  have been prepared by thermal oxidation of a copper surface, cathodic arc deposition of copper in an oxygen atmosphere, chemical vapour deposition of precursors, spray-pyrolysis deposition, electro deposition, plasma evaporation and oxygen-plasma assisted molecular beam epitaxy.

## 7. ZnO AS A PHOTOCATALYST

Next to titania ZnO being explored as a photocatalyst for efficient applications. ZnO has many advantages over titania owing to its efficiency under visible light. The studies based on the synthesis and applications of ZnO based catalysts were reviewed in the forthcoming paragraphs.

The comparison of zinc oxide nanoparticles and its nanocrystalline particles on the photocatalytic degradation of methylene blue was studied by Younh Joon Jang et al (2005) [21]. They synthesized ZnO nanoparticles and ZnO nano-crystalline particles by flame spray pyrolysis methods. They evaluated photocatalytic activity of ZnO nano particles and ZnO nano crystalline particles by measuring the photocatalytic degradation of methylene blue in water under the illumination of UV light. They observed the higher degree of degradation of methylene blue was obtained at the higher concentration of the photocatalysts was employed in reaction. The efficiency of photocatalytic degradation of methylene blue increased with increase in photocatalyst loading and decrease in initial concentration regardless of particle morphology.

Jianguo Yu and Xiaoxiao Yu (2008) studied the hydrothermal synthesis and photocatalytic activity of zinc

oxide hollow spheres [22]. They fabricated ZnO hollow sphere with porous crystalline shells by one-pot hydrothermal treatment of glucose/ $\text{ZnCl}_2$  mixtures at  $180^\circ\text{C}$  for 24h and then calcined at different temperatures for 4h. They evaluated the photocatalytic activity of samples by photocatalytic decolorization of Rhodamine B aqueous solution at ambient temperature. They indicated that the average crystalline size, shell thickness, specific surface areas, pore structures and photocatalytic activity of ZnO hollow spheres could be controlled by varying the molar ratio of glucose to zinc ions(R-molar ratio). They suggested increasing R; the samples show blue shift in the band gap transition, indicating the decrease n crystalline size. They also reported increasing R, increase in the bandgap energy of ZnO. This shift is caused by strengthening of the quantum confinement of charge carriers at decrease in the size of ZnO nanocrystalline particles.

Dorna Mohamad Shahi et al (2017) studied the microemulsion synthesis, optical and photocatalytic properties of vanadium doped nano ZnO [23]. They prepared vanadium doped ZnO nanoparticles with different V concentrations by microemulsion method. They observed that when vanadium doping concentration increased to 5%, the band gap increases in comparison to 1% V-doped ZnO and reaches to 3.25 eV which may be attributed to increase in V doing concentration from optimal level. When V enters into the ZnO lattice, the different ionic radii of V ions distort crystal structure of ZnO. They reported photocatalytic activity of a catalyst depends on different factors such as the crystallinity of the powders, surface OH groups or surface charge, surface area etc. They observed nanoparticles are composed of cubic and rod like nanoparticles. Band gap energy of ZnO reduced from 3.3 eV to 3.21 eV with adding 1% V. They prepared V doped ZnO photocatalyst prepared with 1% V, calcined at  $550^\circ\text{C}$  showed the highest photocatalytic activity among all the samples. They achieved 98% photodegradation of MB under irradiation of UV light for 90 min.

The visible light photocatalytic degradation of 4-chlorophenol using C/ZnO/CdS nanocomposite was studied by Lavand and Malghe (2015) [24]. They prepared the C/ZnO/CdS nanocomposite using the microemulsion method. They confirmed the composite have the cubic CdS and wurzite ZnO phase from XRD studies. They also reported the C/ZnO/CdS nanocomposite consists of a mixture of flakes (C/ZnO) and spherical particles (CdS). They also reported CdS

nanoparticles are successfully deposited on the surface of C doped ZnO nanorods. The length of the C doped ZnO nanorods decreased to 110 nm and width increased to 40 nm due to the deposition of CdS nanoparticles on its surface. They observed C-doped ZnO exhibits a red shift and extends the absorption edge from UV to visible region, the composite having band gap of 2.69 eV. They also observed CdS loading effectively increase the photo absorption capacity of c doped ZnO nanorods in the visible region. They calculated band gap energies of pure and C doped ZnO, pure CdS and C/ZnO/CdS are 3.08, 2.47, 1.98 and 2.20 eV respectively from Kubelka-Munk equation. They observed C/ZnO/CdS nanocomposite exhibits better visible light photocatalytic activity for degradation of 4-CP as compared to bare as well as C doped ZnO. C/ZnO/CdS nanocomposite is a highly stable and reusable photocatalyst.

ZnO is an effective and well known semiconductor with band gap energy of 3.37 eV and has been widely used as an active catalyst with relatively suitable efficiency for the photodegradation of organic pollutants.

## 8. GALLIUM BASED CATALYSIS

As gallium belongs to group 13 (i.e. Boron group) has the flexibility to form varying morphologies in the nanoscale. Inorganic semiconductor nano materials have been considered to be promising for photocatalyst applications because they provide good physical and chemical properties with large surface area, and a variety of morphologies, such as nano rods, cubes, spheres and flowers could be achieved by the chemical synthesis. The subsequent paragraphs will review latest developments in gallium based photocatalysts.

Che-Chia Hu and Hsisheng Teng (2010) studied the oxynitride photocatalysts synthesized from  $\text{Ga}(\text{OH})_3$  for water splitting under visible light irradiation [25]. They synthesized wurtzite-like gallium oxynitride (GaON) photocatalysts by nitridation of  $\text{Ga}(\text{OH})_3$  with  $\text{NH}_3$  at temperatures between 550 and 900°C. They suggested  $\text{Ga}(\text{OH})_3$  precursor more readily converted to wurtzite-phase GaON than  $\text{Ga}_2\text{O}_3$ , probably due to its unoccupied 2-coordinate interstices allowing facile ionic transportation during nitridation. They observed the hybridization of Ga, N and O orbitals, and p-d repulsion between  $\text{N}_{2p}$ ,  $\text{O}_{2p}$  and  $\text{Ga}_{3d}$  hybridized orbitals in valence state in GaON. The repulsion increased the maximum energy of the valence band. They also observed that the band gap energy was minimum for the GaON catalyst with nitridation at 700°C, which gave an N/O atomic ratio close to unity and a high degree of orbital

hybridization. They suggested the degree of orbital hybridization is the primary factor governing the photocatalytic activity of the GaON compounds, while the defect type, either anionic or cationic, superimposes on the primary factor to tune individual  $\text{H}_2$  or  $\text{O}_2$  gas evolution.

The photocatalytic hydrogen evolution from water using copper gallium sulfide under visible light irradiation was reported by Masashi Tabata et al (2010) [26]. They prepared copper gallium sulfide ( $\text{CuGa}_3\text{S}_5$ ) by a solid-state reaction. They investigated  $\text{CuGa}_3\text{S}_5$  exhibits photocatalytic hydrogen evolution activity in an aqueous solution containing  $\text{Na}_2\text{S}$  and  $\text{Na}_2\text{SO}_3$  as sacrificial electron donors under visible light irradiation. They estimated the absorption edge of  $\text{CuGa}_3\text{S}_5$  was approximately 520 nm and the band-gap energy is 2.4 eV. They observed that the photogenerated electrons are able to migrate to NiS suspended in the reactant solution to reduce water, while the holes are scavenged by  $\text{S}^{2-}$  and  $\text{SO}_3^{2-}$  ions. They suggested that the electrochemical measurements and photocatalytic reactions NiS suspended in the reactant solution accepts electron from the excited state of  $\text{CuGa}_3\text{S}_5$  to reduce  $\text{H}^+$  into  $\text{H}_2$  when NiS and  $\text{CuGa}_3\text{S}_5$  particle collide with each other in the reactant solution.

Sivananda Reddy et al (2015) studied the hydrothermal synthesis and photocatalytic property of  $\beta$ - $\text{Ga}_2\text{O}_3$  nanorods [27]. They prepared Gallium oxide ( $\text{Ga}_2\text{O}_3$ ) nanorods by a simple hydrothermal synthesis. They evaluated photocatalytic activity of  $\alpha$  and  $\beta$ -  $\text{Ga}_2\text{O}_3$  for the photodegradation of Rhodamine B solution under UV irradiation. They calcined  $\text{GaOOH}$  nanorods at different temperatures of 500 - 1000°C for converting into single crystalline  $\alpha$ - $\text{Ga}_2\text{O}_3$  and  $\beta$ - $\text{Ga}_2\text{O}_3$  nanorods. They observed at 1000°C of calcinations temperature, the  $\beta$ -  $\text{Ga}_2\text{O}_3$  nanorods with good crystallinity and porous surface formed by the removal of water molecules during the dehydration. They also observed  $\beta$ - $\text{Ga}_2\text{O}_3$  nanorods provides a relatively stable and high photocatalytic activity compared with the  $\alpha$ - $\text{Ga}_2\text{O}_3$  nanorods under UV irradiation the  $\beta$ - $\text{Ga}_2\text{O}_3$  nanorods exhibits a relatively high photodegradation efficiency of 79% compared to the  $\alpha$ - $\text{Ga}_2\text{O}_3$  nanorods (62%).

The sonochemical assisted solvothermal synthesis of gallium oxynitride nanosheets and their solar-driven photoelectrochemical water-splitting applications was studied by Naseer Iqbal et al (2016) [28]. They synthesized gallium oxynitride nanosheets by direct

solvothermal approach. They calculated band energy is  $\sim 1.9$  eV. The reduction of band gap energy is attributed to incorporation of nitrogen and the existence of Ga 3d and N 2p orbitals in the upper valence band of GaON that encouraged more p-d repulsions hence caused an upward shift in its valence band. They reported the photo electrochemical properties of GaON materials enhanced by doping different other metals with GaON via physical methods or incorporation of certain co-catalyst in GaON nanosheets by chemical process.

Galium oxide nanostructures have been recognized as an important material for several applications including catalysts, gas sensors, solar cells and photo detectors due to their wide band gap energy of 4.2 to 4.7 eV and good luminescence properties.

## 9. ZIRCONIUM BASED PHOTOCATALYSTS

In the last few years  $ZrO_2$  mixed material have been intensively studied for enhanced photocatalysis. Presence of a low amount of zirconium oxide (10%) helps in the phase stabilization and maintains the porous structure even at higher calcination temperatures in comparison to pure titania.

Noor Aman et al (2010) studied the facile synthesis of mesoporous N doped zirconium titanium mixed oxide nanomaterial with enhanced photocatalytic activity under visible light [29]. They synthesized high surface and thermally stable N-doped zirconium titanium mixed oxide. They evaluated photocatalytic activity of zirconium titanium mixed oxide nanomaterials by reduction of selenium (VI) to metallic  $Se^0$  under visible light. They observed the pure TiZr material shows a nearly spherical shape of the particles having an average diameter of 50 nm. They also observed that the amount of nitrogen doping and the visible light absorption capacity of the materials increase with the increasing hydrazine amount up to an optimum value. They suggested N-doped titania zirconia material exhibits high surface area and enhanced visible light mediated photocatalytic activity in comparison to nitrogen doped pure titania. They reported are enhanced photocatalytic reduction activity of N-doped titania zirconia mixed oxide under visible that light can be attributed to the synergistic effect of high surface area, presence of oxygen vacancies and substantial N-doping. They also reported an enhanced visible light photocatalysis results of the synthesized materials which may generate significant interest for waste water treatment under visible/solar light.

The photocatalytic activity of combustion synthesized  $ZrO_2$  and  $ZrO_2$ - $TiO_2$  mixed oxides was studied by Sneha

Polisetti et al (2011) [30]. They synthesized tetragonal  $ZrO_2$  by solution combustion technique. They evaluated the photocatalytic activity for the degradation of anionic dyes. The catalyst showed high activity for a very wide range of pH from 3 to 12 for ACG and the 50%  $ZrO_2$ - $TiO_2$  mixed oxides shows activity that comparable to the activity of  $TiO_2$ . The band gap of synthesized  $ZrO_2$  was higher than the commercial  $TiO_2$  and therefore exhibits lesser photocatalytic activity than  $TiO_2$ . They suggested that the presence of  $H_2O_2$ , ranging from 3 to 150 mM, the degradation rates of ACG greatly enhanced. They reported that the conditions of high activity over a large pH range as well as the absence of inhibitory effects due to inorganic salts are highly favorable for industrial applications.

Sulaiman N Basahel et al (2015) studied the influence of crystal structure of nanosized  $ZrO_2$  on photocatalytic degradation of methyl orange [31]. They synthesized nanosized  $ZrO_2$  powders with near pure monoclinic, tetragonal and cubic structures by various methods. They evaluated the photocatalytic active of nanosized  $ZrO_2$  by degradation of methyl orange under UV light irradiation. The photocatalytic activity of the pure monoclinic  $ZrO_2$  sample is higher than that tetragonal and cubic  $ZrO_2$  under optimum identical conditions. They reported that the monoclinic  $ZrO_2$  nanoparticles possessed high crystallinity and mesopores with diameter of 100Å. The photocatalytic activity of m- $ZrO_2$  catalyst mainly attributed to combining effects of factors including the presence of small amount of oxygen-deficient zirconium oxide phase, high crystallinity, broad pore size distribution, and high density of surface hydroxyl group.

The evaluation of the photocatalytic ability of a sol-gel derived MgO- $ZrO_2$  oxide material was studied by Filip Ciesielczyk et al (2017) [32]. They prepared MgO- $ZrO_2$  oxide by sol-gel method. They changed the molar ratio of Mg:Zr and by applying additional heat treatment, the prepared materials with unique properties such as large surface area and porosity or with the formation of a crystalline phase. They observed that the increased the quantity of zirconia in the MgO- $ZrO_2$  oxide material structure affects its properties. The synthesized oxide material was good adsorption ability with respect to the analyzed organic dye (C.I. Basic Blue 9). MgO- $ZrO_2$  oxide materials act as both adsorbents and photocatalysts, designed for the removal of colored impurities from water. The total dye removal varied in the range of 50-70% and strongly dependent on process parameters such

as quantity of photocatalyst, time of irradiation and the addition of promoters.

ZrO<sub>2</sub> has been considered as a photocatalyst in different chemical reactions due to its relatively wide band gap value and the high negative value of the conduction band potential. The ZrO<sub>2</sub> has three polymorphs such as monoclinic, tetragonal and cubic. Preparation methods play an important role in determining the final crystal structure of ZrO<sub>2</sub>.

## 10. PALLADIUM BASED PHOTOCATALYSIS

Palladium metal in nanometer scale dimensions has shown great interest due to it is excellent catalytic ability. Pd particles can serve as a bridge between homogeneous and heterogeneous catalysis and provide new opportunities for catalysis. The following paragraphs will review the latest developments in palladium based photocatalysis.

Christophe Desmaret et al (2007) studied the naphthidine di (radical cation)s- stabilized palladium nanoparticles for efficient catalytic Suzuki-Miyaura cross-coupling reactions [33]. They prepared the stable Pd(0) nanoparticles at room temperature in 1,4-dioxane from PdCl<sub>2</sub> using N,N'-bis(4-methoxyphenyl)-(1,1'-binaphthyl)-4,4' diamine(naphthidine) as reducing and stabilizing agent. They developed a novel and efficient catalyst system for the Suzuki-Miyaura reaction by using naphthidine di(radical cation)s- stabilized palladium nanoparticles as catalyst and K<sub>3</sub>PO<sub>4</sub> as base in dioxane. Pd(0) nanoparticles possessing an average diameter of 25 nm were in situ generated by reduction of PdCl<sub>2</sub> with the naphthidine. They also explained the organic/inorganic material thus produced was found air-and moisture stable allowing the reactions to be conducted under aerobic conditions. The cross coupling of aryl boronic acids with aryl bromides and aryl iodides gave the corresponding biaryl products in excellent yields under the present conditions.

The microwave-assisted of palladium nanocubes and nanobars were studied by Yanchun Yu et al (2009) [34]. They synthesized the palladium nanocubes and nanobars with a mean size of about 23.8 nm were readily synthesized with H<sub>2</sub>PdCl<sub>4</sub> as a precursor, tetra ethylene glycol (TEG) as both a solvent and a reducing agent in the presence of PVP and CTAB in 80s under microwave irradiation. They also observed the presence of the two distinct spots, corresponding to the planes of fcc Pd, indicates that the as-prepared Pd nanocubes are single crystalline structure from TEM images studies. They studied the effect of CTAB on the shape of palladium

nanoparticles by using KBr, KCl or CTAB instead of CTAB in the reaction system. The coordinated ion PdBr<sub>4</sub><sup>2-</sup> was formed due to the coordination replacement of the ligand Cl<sup>-</sup> ions in PdCl<sub>4</sub><sup>2-</sup> ions by Br<sup>-</sup> ion after the addition of bromide, while the addition of CTAB or KCl didn't bring about any change of ligand.

Siamaki et al (2010) studied the micro-wave assisted synthesis of palladium nanoparticles supported on graphene: A highly active and recyclable catalyst for carbon-carbon cross coupling reactions [35]. They generated highly active Pd nanoparticles supported on graphene by microwave-assisted chemical reduction of the corresponding aqueous mixture of palladium nitrate and dispersed graphite oxide sheets. The catalytic activity of Pd/G with a turnover number (TON) of 9000 and turnover frequency (TOF) of 108,000 h<sup>-1</sup>, this is one of the highest turnover frequency observed in a microwave-assisted Suzuki cross-coupling reactions by a Pd nanoparticles catalyst. They also observed the reactivity of the Pd/G catalyst toward Suzuki cross-coupling reactions is attributed to the high degree of the dispersion and concentration of Pd (0) nanoparticles supported on graphene sheets with small particle size of 7-9 nm due to an efficient microwave-assisted reduction method. Both Pd/G and Pd/GO demonstrated excellent catalytic activity for the C - C cross-coupling reactions under ligand-free ambient conditions in an environmental friendly solvent system. These catalysts offer a number of advantages such as high stability of the catalyst, easy removal from the reaction mixture, reusability of the catalyst for eight times with minimal loss of activity and significantly better performance than the well known commercial Pd/C catalyst.

The sonoelectrochemical fabrication of Pd-graphene nanocomposite and its application in the determination of chlorophenols was studied by Jian-Jun Shi and Jun-Jie Zhu (2011) [36]. They synthesized the pd-graphene nanocomposite by sonoelectro chemical method, which exhibited high electrocatalytic activity for chlorophenol oxidation. They proposed the possible formation process driven by the electric and ultrasonic pulses. They also prepared 1L-Pd-graphene nanocomposite, which exhibited remarkable current enhancement and good stability in the determination of CPs. The Pd nano spheres comprised of small Pd nanoparticles were uniformly attached on graphite sheets, Pd-graphene nanocomposite had high activity for chlorophenol oxidation and 2-chlorophenol which was selected as the model molecules. The peak current in linear with the

concentration of phenol in the range from 4 to 800  $\mu\text{mol L}^{-1}$ , and the detection limit is 1.5  $\mu\text{mol L}^{-1}$ . The nanocomposite with large electrochemical active surface led to the excellent electrocatalytic activity and ionic liquid further enhanced the catalytic activity of Pd-graphene for chlorophenols.

Jung et al (2009) studied the performance of carbon nanomaterial (nano tubes and nanofibres) supported platinum and palladium catalysts for the hydrogenation of cinnamaldehyde and of 1-octyne [37]. They synthesized the multi-walled carbon nanotubes as well as the herringbone type carbon nanofibres house in a quartz glass fluidized bed reactor via chemical vapour deposition. The standard Pt/activated charcoal catalyst from Fluka featured a rather homogeneous distribution of the metal with particle diameter of around 50 nm and commercial material Pt/alumina from Aldrich showed metal agglomerates between 5 and 100 nm with the smaller particle fraction dominating. They observed the dispersion degrees ranged from 6% in case of the Pt/multi-walled catalyst and up to 99% for the commercial Pt/activated charcoal material. In the case of platinum catalysts with carbon supports caution is advisable in terms of surface diffusion of hydrogen. The main products 1-octene and n-octane the isomers 2- & 4-octene were formed as by products in the hydrogenation of 1-octyne. The Pd/activated charcoal material generated as a side product most extensively with a selectivity of 37% at a conversion of 97%. The Pd/platelet catalyst, the Pd/herringbone catalyst and the Lindlar material show comparable activities of around 5  $\text{mol}/(\text{kg}_{\text{Pd}}\text{S})$ .

Synthesised Pt and Pd nanosheaths on multi-walled carbon nanotubes as potential electrocatalyst for low temperature fuel cells was studied by Shuangyin Wang et al (2009)[38]. They prepared Pt and Pd nanosheaths on multi-walled carbon nanotubes (MWCNTs) using the nano-covalent poly(diallyl dimethylammonium chloride) (PDDA) functionalization and seed-mediated growth methods. They also observed this method; negatively charged Pt or Pd metal precursors were self-assembled with positively charged PDDA-MWCNTs, forming uniformly distributed Pt or Pd nanoseeds on MWCNTs supports. They explained the non-covalent PDDA-functionalized MWCNTs and the seed-mediated growth method is principle applied for the synthesis of contiguous and porous binary noble metal nanosheath e.g., Pd on Pt on Au on Pt, on carbon nanotube templates. The Pt and Pd nanosheaths structured

catalysts showed the high activities towards the methanol and formic acid oxidation in acid solution respectively, as compared with conventional Pt/C and Pd/C catalysts. They observed a reduced oxophilicity and thus the weakened chemisorptions energy with oxygen-containing species such as  $\text{CO}_{\text{ad}}$ . Adsorbed  $\text{CO}_{\text{ad}}$  species are generally formed as intermediate during the methanol and formic acid electrooxidation on Pt catalysts. The existence of large amounts of grain boundaries in the nanosheath structure, which could act as the active sites for fuel oxidation reactions.

Xiangjie Bo et al (2011) studied the nanocomposite of PtPd nanoparticles/onion-like mesoporous carbon vesicle for nonenzymatic amperometric sensing of glucose [39]. They introduced PtPd bimetallic alloy nanoparticles on the onion-like MCV by microwave assisted reduction method. The PtPd/MCV nanocomposite exhibits enhanced current response towards the direct oxidation of glucose and gives linear range from 1.5 to 12mM. They reported MCV is mostly nanoporous material with quite narrow pore size distribution centered at 5.3 and MCV possesses BET are of 569  $\text{m}^2\text{g}^{-1}$  and large pore volume of 0.84  $\text{cm}^3\text{g}^{-1}$ . They reported the addition of Pd to Pt leads to a decrease in the lattice parameters of PtPd/MCV. They also observed that direct glucose oxidation is catalyzed more easily on PtPd nanoparticles than on Pt nanoparticles. The Pt(25)Pd(25)/MCV/Nafion/GC electrode displays the better performance due to either an electronic effect or the bifunctional mechanism. The onion-like structure and high surface area of the MCV allow for the obtainment of high dispersed PtPd nanoparticles. Nanoscale PtPd particles may supply more surface active sites for the adsorption of reactants.

Pd nano catalysts exhibited high electro catalytic activity for the oxidation of phenolic compounds. Pd(0) nanoparticles have been developed for carbon-carbon bond forming reactions and especially for Suzuki-Miyaura and Hiyama couplings.

## 11. TIN BASED CATALYSIS

Tin oxide is one of the most important semiconductor oxides.  $\text{SnO}_2$  used as photocatalyst for photodegradation of many organic compounds. The  $\text{SnO}_2$  photocatalyst is used widely and practically in the environmental applications.

The synthesis, characterization and activity of tin oxide nanoparticles: Influence of solvothermal time on photocatalytic degradation of Rhodamine B was studied by Zuoli He and Jiaqi Zhou (2013) [40]. They synthesized

SnO<sub>2</sub> nanoparticles by a microwave solvothermal method. They investigated the photocatalytic activity of SnO<sub>2</sub> nanoparticles by the degradation of Rhodamine B under UV-light illumination. They observed SnO<sub>2</sub> nanoparticles with diameter about 1-2 μm, and when the reaction time prolong, the surface of the SnO<sub>2</sub> spheres will change to rough and then smooth when the time even longer. They also observed the product with nanorods on its surface shows the higher photocatalytic activity and red shift in the UV-Visible absorption, which are relative to the unique structure. They reported the RhB interact with the photogenerated holes in the valence band and provides a direct chemical reaction between the dye and the photocatalyst.

Ganesh Elango et al (2015) studied the green synthesis of SnO<sub>2</sub> nanoparticles and its photocatalytic activity of phenolsulfonphthalein dye [41]. They prepared tin oxide nanoparticles using Persia Americana seeds methanolic extract by calcining stannous chloride precursors at 300-500°C by green synthesis method. They observed SnO<sub>2</sub> nanoparticles size of 4 nm in range. They evaluated photocatalytic activity of SnO<sub>2</sub> nanoparticle by photodegradation of phenolsulfonphthalein dye under UV irradiation. On illumination of catalyst (SnO<sub>2</sub>NPs) surface with enough energy, leads to the formation of a hole (h<sup>+</sup>) in the valence band and the electron in the conduction band. The hole oxidizes either pollutant directly or water to produce OH<sup>·</sup> radicals, the electron in the conduction band reduce the oxygen adsorbed on the catalyst. They also reported green synthesized SnO<sub>2</sub> nanoparticles totally degraded in one of the toxic organic dyes (phenol red).

The enhancement of photocatalytic activity of tin oxide by nitrogen doping was studied by Kavita Ranawat et al (2015) [42]. They prepared nitrogen doped tin oxide by precipitation method through doping pure SnO<sub>2</sub> with urea. They also studied dye degradation from different rate affecting parameters like pH, dye concentrations, catalyst amount and light intensity. The rate of photocatalytic degradation of new fuchsin increased with increased pH and attained optimum value at pH 9.5 and also further increased pH the rate was decreased. The rate of photocatalytic degradation of dye was increased on increasing concentration of new fuchsin up to 3.80<sup>-5</sup> M and rate of degradation decreased with increasing the concentration of dye above 3.80<sup>-5</sup> M. They reported the nitrogen doped SnO<sub>2</sub> shows higher activity than the pure SnO<sub>2</sub> under visible light irradiation.

Pham VanViet et al (2016) studied the high photocatalytic activity of SnO<sub>2</sub> nanoparticles synthesized by hydrothermal method [43]. They prepared tin oxide nanoparticles at low temperature by hydrothermal method. They evaluated the synthesized nanoparticle size was 3 nm and they have high photocatalytic activity. They reported very small amount of SnO<sub>2</sub> nano particles; 10.03 g was degradable more over 90% MB solution under UV illumination condition for 2h. They also reported SnO<sub>2</sub> nanoparticles degraded 88.88% MB solution after 30 minutes of UV illumination and reached 90.0% for 120 minutes of UV illumination and also degraded 79.26% MB solution after 90 minutes under assisted sunlight illumination.

SnO<sub>2</sub> nano particles have several morphologies like nanorods, nanowires, nanotubes, hollow spheres, mesoporous structures. Based on the morphologies of SnO<sub>2</sub>, the potential applications of the synthesized nano particles varies, one of them is sensors, which produces the signal proportional to gas concentration.

## 12. OTHER LANTHANUM TRANDITION METAL BASED CATALYSIS

Lanthanum oxide has different applications such as synthesis of ferroelectric and optical materials. It has the lowest lattice energy of the rare earth oxides with very high dielectric constant of 27. It shows a p-type semi conducting property. Its resistivity at ambient temperature is equal to 10 kcm. Lanthanum oxide is used to make optical glasses, which increases their density, refractive index and hardness. It is also used as a catalyst for the oxidative coupling of methane. The following paragraphs review the various preparative methods of lanthanum based catalysts and their applications.

The synthesis, characterization and photocatalytic properties of lanthanum oxy-carbonate, lanthanum oxide and lanthanum hydroxide nanoparticles was studied by Mahnaz Ghiasi and Azim Malekzadeh (2014) [44]. They prepared La<sub>2</sub>O<sub>3</sub> and La<sub>2</sub>O<sub>2</sub>CO<sub>3</sub> nanoparticles. The effect of citric acid as emulsifier on the particle size and thermal properties of the obtained product was negligible, confirming emulsifier free advantage. They also reported the thermal decomposition of precursor at 700°C for 5h leads to the formation of lanthanum oxy-carbonate with average size of ~35 nm. They evaluated the photocatalytic behavior of samples using the degradation of a methyl orange aqueous solution under UV light irradiation. They also reported a pseudo-first order kinetic obtained for the photocatalytic degradation of

methyl orange over  $\text{La}_2\text{O}_2\text{CO}_3$  nanoparticles according to the Langmuir-Hinshelwood analysis.

Huan Liu and Zhen Ma (2016) investigated the effect of different  $\text{LaPO}_4$  supports on the catalytic performance of  $\text{Rh}_2\text{O}_3/\text{LaPO}_4$  in  $\text{N}_2\text{O}$  decomposition and CO oxidation [45]. They synthesized four  $\text{LaPO}_4$  supports by different preparation methods.  $\text{LaPO}_4$  used to support  $\text{Rh}_2\text{O}_3$  via impregnation using  $\text{Rh}(\text{NO}_3)_3$  as a precursor. They also showed the most active  $\text{Rh}_2\text{O}_3/\text{LaPO}_4$ -HNW catalyst has highly dispersed  $\text{Rh}_2\text{O}_3$  species, the strongest  $\text{Rh}_2\text{O}_3/\text{LaPO}_4$  interaction, as well as the largest amount of basic sites and  $\text{O}_2$ -adsorption sites.

The ultrathin lanthanum tantalite perovskite nano sheets modified by nitrogen doping for efficient photocatalytic water was studied by Meilin Lv et al (2017) [46]. They successfully fabricated ultrathin  $\text{LaTa}_2\text{O}_{6.77}\text{N}_{0.15}$  nano sheets by exfoliating nitrogen doped DJ type perovskite compound  $\text{RbLaTa}_2\text{O}_7$ . These nanosheets are typical 2D semiconductors with perovskite structure and strong visible light absorption as far as 600nm. They also observed intense light absorption stems from the hybridization between  $\text{O}_{2p}$  and  $\text{N}_{2p}$  orbitals which considerably uplift the valence band maximum. They reported pristine  $\text{RbLaTa}_2\text{O}_7$  is a typical wide band gap semiconductor with band gap as large as 4.2 eV, such large band gap essentially prevents it from usage in solar energy conversions due to limited light absorption. They showed apparent quantum efficiency under visible light illumination which approaches 1.29% and 3.27% for photocatalytic hydrogen and oxygen production with almost 4 fold and 8 fold higher than their bulk counterpart.

Gajendra Kumar Pradhan and K.M.Parida (2010) studied the fabrication of iron-cerium mixed oxide: an efficient photocatalyst for dye degradation [47]. They synthesized the mesoporous and nano structured iron-cerium mixed oxides for photodegradation of phenol, methylene blue and congo red by direct illumination to sun light. They observed a mixed phase of two opposite character catalyst compensate with the synergistic effect to become an efficient photocatalysts. They also observed ceria and its mixed oxides containing higher percentage of cerium can only utilize UV light (4% of solar light) for photo degradation of dyes. The mixed oxides enhanced surface acidity compared to single component and also enhance the photocatalytic activity. They also observed complete mineralization of CR, the reason for higher catalytic activity of 1:1 (Fe/Ce) sample has higher surface area,

surface acidity which determines the active sites of the catalyst and accelerates the photocatalytic reaction.

The preparation, characterization, photocatalytic properties of hollow titania doped with cerium was studied by Chao Wang et al (2010) [48]. They prepared Ce-doped titania using carbon spheres as template and Ce-doped titania nanoparticles as building blocks. They also prepared Ce-doped titania nanoparticles at low temperature. They showed that the Ce doping causes a red-shift of absorption spectrum for titania. They also investigated the effect of Ce content on the physical structure and photocatalytic properties of doped titania sphere samples. The photocatalytic activity of hollow titania spheres with different Ce-doped content was determined by degradation of Reactive Brilliant Red dye X-3B under visible light irradiation. They reported Ce-doped titania hollow spheres samples are all with high photocatalytic activity under visible light.

Weiliang Xue et al (2011) studied the preparation of titania nanotubes doped with cerium and their photocatalytic activity for glyphosate [49]. They synthesized  $\text{TiO}_2$  through hydrothermal treatment of rutile phase  $\text{TiO}_2$  nanoparticles in  $10 \text{ mol}^{-1}$  NaOH solution at  $130^\circ\text{C}$  for 24h and cerium doped titania nanotubes prepared by impregnation method. Both  $\text{Ce}^{3+}$  and  $\text{Ce}^{4+}$  coexisted in Ce/ $\text{TiO}_2$  nanotubes and cerium species in  $\text{TiO}_2$  nanotubes influence the photo reactivity by altering the electron-hole pair recombination rate. The cerium doping enhanced the photocatalytic activity of Ce- $\text{TiO}_2$  nanotubes. The glyphosate on Ce- $\text{TiO}_2$  nanotubes was effectively decomposed and the photocatalytic activity of glyphosate is 0.15% for Ce- $\text{TiO}_2$  nanotubes calcined at  $400^\circ\text{C}$ . They also reported Ce- $\text{TiO}_2$  nanotubes have sensing, photovoltaics and catalytic activity because of their hollow cores and high specific surface area.

One pot synthesis of cerium oxide/sulfur-doped graphite carbon nitride ( $\text{g-C}_3\text{N}_4$ ) as efficient nano photocatalysts under visible light irradiation was studied by Milad Jourshabani et al (2017) [50]. They synthesized porous  $\text{CeO}_2$ /sulfur-doped  $\text{g-C}_3\text{N}_4$  ( $\text{CeO}_2/\text{CNS}$ ) composites by one-pot thermal condensation of thiourea and cerium nitrate as starting materials. They reported specific surface area and pore volume of  $\text{CeO}_2$  (9.5)/CNS composite were  $34.9 \text{ m}^2/\text{g}$  and  $0.12 \text{ cm}^3/\text{g}$ , which were approximately 3.9 and 4.9 times greater than those of the pure CNS ( $8.9 \text{ m}^2/\text{g}$  &  $0.026 \text{ cm}^3/\text{g}$ ), respectively. The optimized composite containing 9.5 wt%  $\text{CeO}_2$  exhibited the highest photocatalytic activity (91.4% after 150min)

for the MB degradation under visible light irradiation. The presence of the S dopant within CeO<sub>2</sub>/CNS composite texture created hetero junction between the CNS and the CeO<sub>2</sub> resulting in efficient separation of charge carriers and enhanced photocatalytic activity. They showed the CeO<sub>2</sub>/CNS photocatalyst has high stability after the third reusability experiment without any obvious decrease in its performance under the optimized conditions.

Vincenzo Vaiano et al (2017) studied photocatalytic treatment of aqueous solutions at high dye concentration using praseodymium-doped ZnO catalysts [51]. They prepared Pr-ZnO photocatalysts by precipitation method and it treated the aqueous solutions at high concentration of organic dyes under UV or visible irradiation. They studied ZnO is hexagonal wurtzite phase and that Pr<sup>3+</sup> ions were successfully incorporated into the ZnO lattice. The hair dyeing industry waste water was treated under UV light radiation for 360 minutes, they got complete discoloration and mineralization of basic Red 51 dye using optimized photocatalyst. Moreover, Pr-ZnO samples present band-gap values of about 3.0 eV, lower than undoped ZnO (3.3 eV). The highest enhancement in the photocatalytic activity was achieved by using ZnO doped with 0.46 mol% of Pr[Pr-ZnO(0.46%)] under UV light. They achieved complete removal of the azo dye Eriochrome Black T by UV light passed for 120 minutes. They observed Pr-ZnO (0.46%) sample showed a significant photocatalytic activity under visible light while undoped ZnO was ineffective.

La-doped TiO<sub>2</sub> showed an excellent photocatalytic activity and relative photonic efficiency compared to other photocatalysts. Electron trapping by lanthanum metal ions, smaller particle size, large surface area, high porosity and increase in surface roughness may be the reasons for the enhanced photocatalytic activity. Among the semiconductor CeO<sub>2</sub> as one of the rare earth oxides is of great attention as a result of its unique properties such as its high oxygen storage ability, non toxicity and the valence change between Ce<sup>4+</sup> and Ce<sup>3+</sup> states which can be helpful in retarding the recombination of photo generated electron hole pairs.

### 13. CONCLUSION

There are thousands of composite photocatalysts were tried by the researchers for the effective degradation of textile dyes. Tuning the optical band gap is the main criteria for the effective utilization of generated electron hole pair. In this review, the advantages and drawbacks of Titanium, Vanadium, Manganese, Cobalt, Copper,

Zinc, Gallium, Zirconium, Palladium, Tin and Inner transition metal doped photocatalysts were critically analyzed. This review will serve an effective key for design and fabrication of a novel photocatalytic system.

### 14. REFERENCES

1. Watson S, Beydoun D, Scott J, Amul R, *J Nanoparticle Res*, 2004; **6**: 193-207.
2. Liao DL, Liao BQ, *J photochem Photobiol A: Chem*, 2007; **187**: 363-369.
3. Suresh Kumar BV, Sajan CP, Lokanatha Rai KM, Byrappa K, *Ind J Chem Technol*, 2010; **17**: 191-197.
4. Chang Hyo Kim, Bo-Hye Kim, Kap Seung Yang, *Carbon*, 2012; **50**: 2472-2481.
5. Benxia Li, Yang Xu, Guoxin Rong, Meng Jing and Yi Xie, *Nanotechnol*, 2006; **17**: 2560-2566.
6. Yuquan Wang, Zhengjum Zhang, Yu Zhu, Zhengcao Li, Robert Vajtai, et al. *J Am Chem Soc*, 2008; **2(7)** : 1492-1496.
7. Chiing-Chang C, Janah Shaya, Huan-Jung F, Yi-Kuo C, Han-Ting C and Chung-Shin L, *J Material Sci Eng*, 2007; **6** : 6 -12.
8. Yim-Leng Chan, Swee-Yong Pung and Srimala Sreekantan, *J catal*, **2014**, ID 370696, <http://dx.doi.org/10.1155/2014/370696>
9. Bosi Yin, Siwen Zhang, Yang Jiao, Yang Liu, Fengyu Qu and Xiang Wu, *Cryst Eng Comm*, 2014; **16**: 9999-10005.
10. Safi Asim Bin Asif, Sher Bahadar Khan and Abdullah M Asiri, *Nanoscale Res Let*, 2015; **10**: 355-364.
11. Haile Jasana Logita, Abi Tadesse and Tesfahun Kebede, *African J Pure Appl. Chem.*, 2015; **9(11)**: 211-222.
12. Manoj Pudukudy and Zahira Yaakob, *J Nanoparticles*, 2016, article id 8037013,7, <http://dx.doi.org/10.1155/2016/8037013>
13. Christoffer Johans, Maija Pohjhallio, Mari Ijas, Yanling Ge, Kyosti kontturi, *Physicochem Eng Aspects*, 2008; **330**: 14 – 20.
14. Safi Asim Bin Asif, Sher Bahadarkhan and Abdullah M Asiri, *Nanoscale Res Let* 2014; **9**: 510.
15. David Greene, Raquel Serrano-Garcia, Joseph Govan, Yurii K. Gunko, *Nanomaterials*, 2014; **4**: 331-343.
16. Zhenguo Guo, Siwei Cheng, Claudio Cometto, Elodie Anxolabehere-Mallart, et al., *J Am Chem Soc*, 2016; **138**: 9413.
17. Rashadm MM, Mohamed RM, Ibrahim MA, Ismail LFM, Abdel-Aal EA, *Adv Powder Technol*, 2012; **23**: 315-323.

18. Anshu Singhal, Mrinal R. Pai, Rekha Rao, Kodanthakurup T. Pillai, Ingo Lieberwirth and Avesh K. Tyagi, *European J. Inor.Chem.*, **14**, 2640 (2013), doi:10.1002/ejic.201201382
19. Shababa Afzal, Walid A Daoud, and Steven J. Langford, *ACS Appl Mater Interfaces*, 2013; **5(11)**:4753.
20. Sankar R, Manikandan P, Malarvizhi V, Fathima T, Shivashangari KS, Ravikumar V, *Spectrochimica acta part A: Molecular and Biomolecular spectroscopy*,2014; **121**: 746-750.
21. Jang YJ, Simer C, Ohm T, *Mater Res Bulletin*, 2006; **41**: 67- 77.
22. Jiaguo Yu and Xiaoxiao Yu, *Environ Sci Technol*, 2008; **42**: 4902-4907.
23. Dorna Mohamad Shahi, Hassanzadeh-Tabrizi SA, Saffar-Teluri A, *Int J Appl Ceramic Technol*, 2017; **15(2)**: 479.
24. Atul, Lavand B, Yuvraj, Malghe S, *J Saudi Chem Soc*, 2015; **19**: 471-478.
25. Che-Chia Hu and Hsisheng Teng, *JPhyChemC*, 2010; **114**:20100.
26. Tabata M, Maeda K, Ishihara T, Minegishi T, Takata T, and Domen K, *J Phys Chem C*, 2010; **114**: 11215-11220.
27. Sivananda Reddy L, Yeong Hwan Ko and Jae Su Yu, *Nanoscale Res Let*, 2015; **10**: 364.
28. Iqbal N, Ibrahimkhan, YamaniZH and Qurashi A, *Scientific reports***6**: 32319, Doi:10.1038/srep32319
29. Aman Z, Mishra T, Sahu RK and Tiwari JP, *J Mater Chem*, 2010; **20**: 10876-10882.
30. Poliseti S, Deshpande PA and Madras G, *IndEng Chem Res*, 2011; **50**: 12915-12924.
31. Basahel SN, Ali TT, Mokhtar M and Narasimharao K, *Nanoscale Res Let*,2015; **10**: 73.
32. Ciesielczyk F, Szczekocka W, Siwinska-stefanska K, Piasecki A, et al, *Open Chem*, 2017; **15**: 7-18.
33. Desmarests C, Amrani RO, Walcarius A, Lambert J, et al, *Tetrahedron*,2008; **64**:372-381.
34. Jung A, JessA, Schubert T, Schutz W, *Applied catalysis A: General*, 2009; **362**:95-105.
35. Ali R. Siamaki, Abd EI Rahman S. Khder, Victor Abdelsayed, Samy EI-Shall M, Frank Gupton B, *J Catal*, 2011; **279**: 1-11.
36. Yu Y, Zhao Y, Hueng T, Liu H, *Mater Res Bulletin*,2010; **45**: 159-164.
37. Jian-Jun Shi, Jun-Jie Zhu, *Electrochimica Acta*, 2011; **56**: 6008-6013.
38. Shuangyin Wang, San Ping Jiang, White TJ, Xin Wang, *Electrochemical Acta*,2010; **55**: 7652-7658.
39. Xiangjie Bo, Jing Bai, Li Yang, Liping Guo, *Sensors and Actuators B: Chemical*, 2010; **157**: 662-668.
40. Zuoli He, Jiaqi Zhou, *Modern research in catalysis*, 2013; **2**: 13-18.
41. Elango G, Kumaran SM, Kumar SS, Muthuraja S, Roopan SM, *Spectrochimica Acta Part A: Molecular & Biomolecular Spectroscopy*, 2015; **145**: 176-180.
42. Kavita Ranawat, Chittora AK, Rakshit Ameta and Sanyogita Sharma, *J Curr Chem Pharm Sci*, 2015; **5(4)**: 127-135.
43. Pham Van Viet, Cao Minh Thi, Le Van Hieu, *J Nanomaterials*, 2016, ID 4231046, 8 pages.
44. Ghiasi M, Malekzadesh A, *Superlattices and Microstructures*, 2014; **77**: 295-302.
45. Huan Liu, Zhen Ma, *J. Taiwan Institute of Chemical Eng.*, 2016; **71**: 1-8.
46. Meilin Lv, Xiaoqin Sun, Shunhang Wei, Caishen, Yongli Mi and Xiaoxiang Xu, *ACS Nano*, 2017; **11(11)**: 11441-11448.
47. Pradhan GK, Parida KM, *Int J Eng Sci Technol*, 2010; **2(9)**: 53-65.
48. Wang C, Ao Y, Wang P, Hou J, Qian J, Zhang S, *J Hazard Mater*, 2010; **178**: 517-521.
49. Xue W, Zhang G, Xu X, Yang X, Liu C, Xu Y, *Chem Eng J*, 2011; **167**: 397-402.
50. Jourshabani M, Shariatinia Z, Badiie A, *J Colloid Interf Sci*, 2017; **507**: 59-73.
51. Vaiano V, Matarangolo M, Sacco O, Sannino D, *Applied Catal. B: Environ.*, 2017; **209**: 654-665.